Solid Earth Discuss., https://doi.org/10.5194/se-2019-57
Manuscript under review for journal Solid Earth
Discussion started: 27 March 2019

Solid Earth Discussions
Open Access
EGU

Actors, actions and uncertainties: Optimizing decision making based on 3-D structural geological models

Fabian Antonio Stamm[1], Miguel de la Varga[1,2], and Florian Wellmann[1]

[1]Computational Geoscience and Reservoir Engineering (CGRE), RWTH Aachen University, Germany
[2]Aachen Institute for Advanced Study in Computational Engineering Science (AICES), RWTH Aachen University, Germany

Correspondence: Fabian Antonio Stamm (fabian.stamm@rwth-aachen.de)

Abstract. Uncertainties are common in geological models and have a considerable impact on model interpretations and subsequent decision making. This is of particular significance for high-risk, high-reward sectors, such as hydrocarbon exploration and production. Recent advances allows us to view geological modeling as a statistical problem that we can address with probabilistic methods. Using stochastic simulations and Bayesian inference, uncertainties can be quantified and reduced by incorporating additional geological information. In this work, we propose custom loss functions as a decision-making tool that builds upon such probabilistic approaches.

As an example, we devise a case in which the decision problem is one of estimating the uncertain volume of a structural hydrocarbon trap. We construct a synthetic 3-D model to represent a potential hydrocarbon system and develop algorithms for automatic trap volume calculation. Various volume probability distributions for different information scenarios are attained via Monte Carlo error propagation and Markov chain Monte Carlo sampling. For subsequent true value estimation, we design a case-specific loss function to reflect not only the decision-making environment, but also the preferences of differently risk-affine actors. Based on this function, optimizing for expected loss returns an actor's best estimate to base decision making on.

Our results show that the optimizing estimators shift according to the characteristics of the underlying value distribution. While overall spread leads to separation, risk-averse and risk-friendly decisions converge in the decision space and decrease in expected loss given narrower distributions. We thus consider the degree of decision convergence to be a measure for the state of knowledge and its inherent uncertainty at the moment of decision making. This decisive uncertainty does not change in alignment with model uncertainty but depends on alterations of critical parameters and respective interdependencies, in particular relating to seal reliability. Additionally, actors are affected differently by one set of information, depending on their risk affinity. It is therefore important to identify the model parameters which are most influential for the final decision in order to optimize the decision-making process.

Solid Earth Discuss., https://doi.org/10.5194/se-2019-57
Manuscript under review for journal Solid Earth
Discussion started: 27 March 2019

1 Introduction

In studies of the subsurface, data availability is often limited and characterized by high possibilities of error, as well as epistemic uncertainty, due to signal noise or inaccuracies. This leads to the inevitable presence of significant uncertainty in geological models, which in turn may affect interpretations and conclusions drawn from a model (Wellmann et al., 2018; de la Varga and Wellmann, 2016; de la Varga et al., 2019; Wellmann et al., 2010; Bardossy and Fodor, 2004; Randle et al., 2019; Lark et al., 2013; Caers, 2011; Chatfield, 1995). Uncertainties are thus of particular importance for making responsible and good decisions in related economic settings, such as in hydrocarbon exploration and production (Thore et al., 2002; McLane et al., 2008; Smalley et al., 2008). Quantification and visualization of such uncertainties and their consequences is a currently active field of research. Recent developments allow us to view geological modeling as a statistical problem (see Wellmann and Caumon (2018)). We particularly regard approaches to couple implicit geological modeling with probabilistic methods, as presented by de la Varga et al. (2019) with the Python library GemPy.

Following their example, we regard implicit geological modeling as a mathematical function of not only deterministic but also stochastic, i.e. uncertain, model input parameters. An essential aspect of this approach to modeling is that it allows for full automation, so that the consequences of a change in an input parameter are realized directly without the need for any further manual inspection or interaction (Wellmann et al., 2017; de la Varga and Wellmann, 2016). This not only enables us to quantify model uncertainties using Monte Carlo error propagation, but also allows us to incorporate additional information via Bayesian inference to reduce uncertainties.

Building on this probabilistic perspective, in this work, we propose the use of custom loss functions as a decision-making tool when dealing with uncertain geological models. In many applications, we are interested in some decisive model output value, for example reservoir volume. Given that such a value is the result of a deterministic function of uncertain variables in our model, the value of interest is likewise uncertain and can be represented by a probability distribution attained from stochastic simulations. A loss function can be applied to such a distribution to return a case-specific best estimate to base decision making on.

We consider hydrocarbon exploration and production as an exemplary high-risk, high-reward sector, in which good decision making is crucial. Monte Carlo simulation for reservoir estimation and risk assessment has become common in this sector and is often used in combination with decision trees (see Murtha et al. (1997), Mudford et al. (2000), Wim et al. (2001) and Bratvold and Begg (2010)). However, it seems to us that distributions resulting from probabilistic modeling are mostly only considered to attain best estimates in the form of means. Most likely and extreme outcomes are identified as percentiles, typically P50 (the median), P10 and P90. We believe that this practice does not harness the full potential of such a probabilistic distribution and that much of the inherent information is discarded. Contrary to that, customized loss functions, as a Bayesian method, take into account the full probability distribution and enable the inclusion of various conditions in the process of finding an optimal estimate. While used in statistical decision theory and other scientific fields, loss functions have, to the best of our knowledge, found no significant application in the field of petroleum exploration and production. Thus, we intend to provide a new perspective with our methodology.

Solid Earth Discuss., https://doi.org/10.5194/se-2019-57
Manuscript under review for journal Solid Earth
Discussion started: 27 March 2019

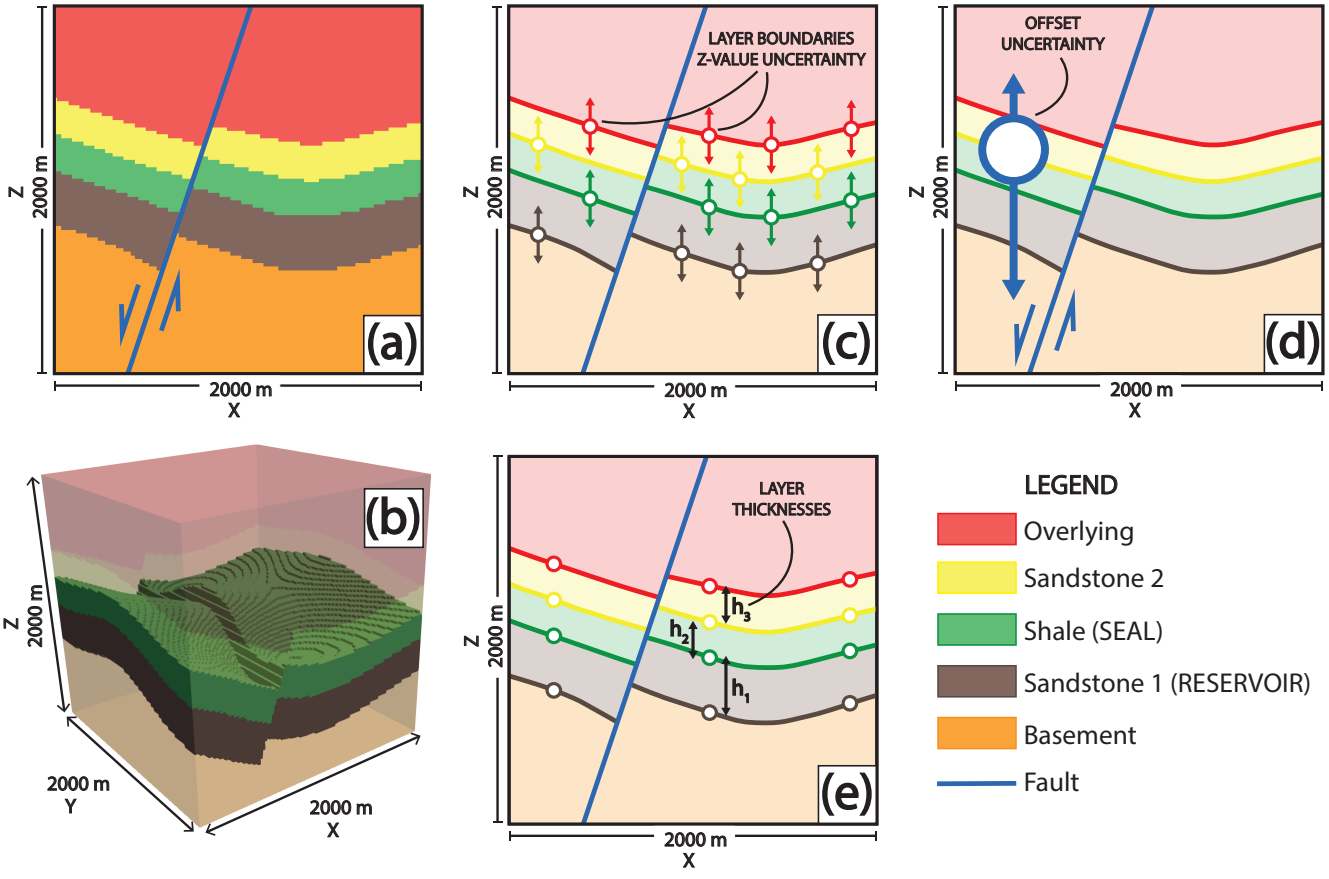

Figure 1. Design of our 3-D structural geological model. A 2-D cross section through the middle of the model (y = 500 m), perpendicular to the normal fault (parallel to the $x - z$ plane), is shown in (a). A 3-D voxel representation of the model, highlighting the reservoir and seal formations, is visualized in (b). In (d) and (d), the inclusion of parameter uncertainties is presented. Colors indicate certain layer bottoms (i.e. boundaries) which are assigned shared z-positional uncertainties (c). All points in the hanging wall are additionally assigned a fault offset uncertainty (d). Thicknesses of the three middle layers are defined by the distances of boundary points (e) and are thus directly dependent on (c).

To illustrate our approach, we apply it to a simple synthetic 3-D geological model that comprises deformed geological units and a normal fault which together form a potential structural hydrocarbon trap. Assuming a petroleum exploration and production case, we define the maximum trap volume as our value of interest. Decision makers would want to best estimate this volume to derive recoverable reserves, economic value and subsequently allocate development resources accordingly.

Solid Earth Discuss., https://doi.org/10.5194/se-2019-57
Manuscript under review for journal Solid Earth
Discussion started: 27 March 2019

2 Methods

2.1 Computational implementation

Computationally and numerically, we implement all out methods in a Python programming environment, relying in particular on the combination of two crucial open source libraries: (1) GemPy (version 1.0) for implicit geological modeling and (2) PyMC (version 2.3.6) for conducting probabilistic simulations.

Gempy is able to generate and visualize complex 3-D structural geological models based on a potential-field interpolation method originally introduced by Lajaunie et al. (1997) and further elaborated by Calcagno et al. (2008). GemPy was specifically developed to enable the embedding of geological modeling in probabilistic machine-learning frameworks, in particular by coupling it with PyMC (de la Varga et al., 2019).

PyMC was devised for conducting Bayesian inference and prediction problems in an open-source probabilistic programming environment (Davidson-Pilon, 2015; Salvatier et al., 2016). Different model-fitting techniques are provided in this library, such as various Markov chain Monte Carlo (MCMC) sampling methods. For our purpose we make use of Adaptive Metropolis sampling by Haario et al. (2001) and check for MCMC convergence via a time-series method approach by Geweke et al. (1991). Components of a statistical model are represented by deterministic functions and stochastic variables in PyMC (Salvatier et al., 2016). We can thus use the latter to represent uncertain model input parameters and link them to additional data via likelihood functions. Other parameters, such as the value of interest for decision making, can be determined over deterministic functions, as children of parent input parameters.

To visually compare the states of geological unit probabilities after conducting stochastic simulations, we consider the normalized frequency of lithologies in every single voxel and visualize the results in probability fields (see Wellmann and Regenauer-Lieb (2012)).

2.2 Synthetic geological model

Our geological example model is designed to represent a potential hydrocarbon trap system. Stratigraphically, it includes one main reservoir unit (sandstone), one main seal unit (shale), an underlying basement and two overlying formations that are assumed to be permeable, so that hydrocarbons could have migrated upwards. Structurally, it is constructed to feature an anticlinal fold that is displaced by a normal fault. All layers are tilted and dip in the opposite direction of the fault plane dip. A potential hydrocarbon trap is thus found in the reservoir rock enclosed by the deformed seal and the normal fault.

Using GemPy, we construct the geological model as follows: In principle, it is defined as a cubic block with an extent of 2000 m in x-, y- and z-directions. The basic input data for the interpolation of the geological features is composed of 3-D point coordinates for layer interfaces and fault surfaces, as well as orientation measurements that indicate respective dip directions and angles. From this data, GemPy is able to interpolate surfaces and compute a voxel-based 3-D model (see Fig. 1).

We include uncertainties by assigning them to the z-positions of points which mark layer interfaces in the 3-D space. This is achieved via probability distributions (PyMC stochastic variables) from which deviation values are drawn. These are then added to the original input data z-value. As the z-position is the most sensible parameter for predominantly horizontal layers, we can

Solid Earth Discuss., https://doi.org/10.5194/se-2019-57
Manuscript under review for journal Solid Earth
Discussion started: 27 March 2019

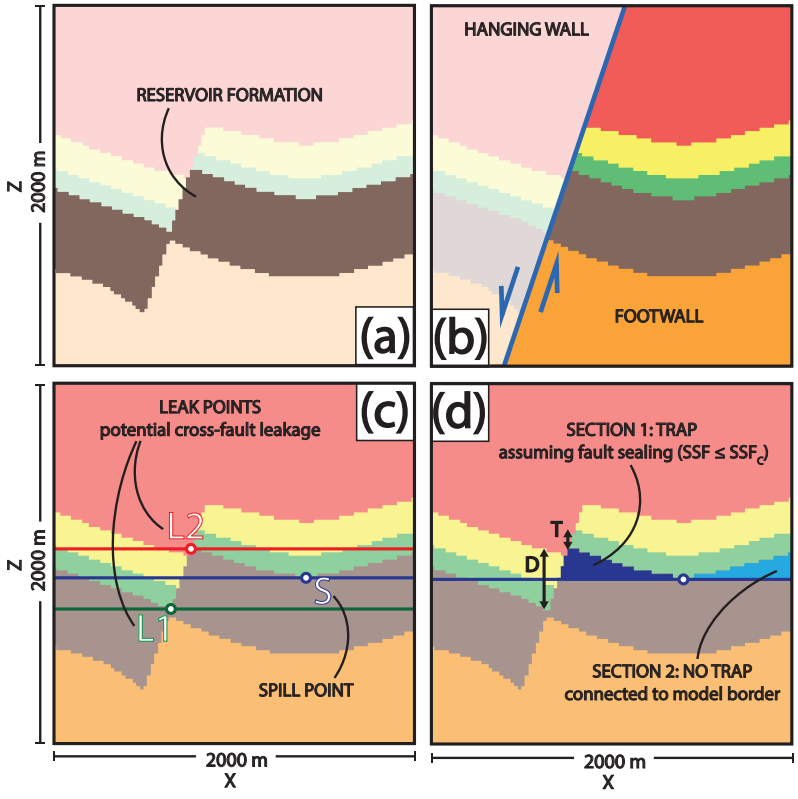

Figure 2. Illustration of the process of trap recognition in 2-D, i.e. the conditions that have to be met by a model voxel, to be accepted as belonging to a valid trap. A voxel has to be labeled as part of the target reservoir formation (a) and positioned in the footwall (b). Trap closure is defined by the seal shape and the normal fault (c). Consequently, the maximum trap fill is defined by either the anticlinal spill point (S) or a point of leakage across the fault, depending on juxtapositions with layers underlying (L1) or overlying the seal (L2). The latter is only relevant if the critical Shale Smear Factor is exceeded, as determined over D and T in (d). In this example, assuming sealing of the fault due to clay smearing, the fill horizon is determined by the spill point in (d). Subsequently, only trap section 1 is isolated from the model borders in (d) and can thus be considered a closed trap. Voxels included in this section are counted to calculate the maximum trap volume.

Solid Earth Discuss., https://doi.org/10.5194/se-2019-57
Manuscript under review for journal Solid Earth
Discussion started: 27 March 2019

Table 1. Input parameter uncertainties defined by distributions with respective means μ, standard deviations σ and shape factor α.

	mu	sigma	alpha
Overlying	0	40	0
Sandstone 2	0	60	0
Seal	0	80	0
Reservoir	0	100	0
Fault offset	0	-150	-2

hereby not only implement uncertainties regarding layer surface positions in depth, but also layer thicknesses, geometrical shapes and degree of fault offset.

Such probability distributions can also be allocated as homogeneous sets to point and feature groups which are to share a common degree of uncertainty (see Table 1). We assign the same base uncertainty to groups of points belonging to the same layer bottom surface by referring them to one shared distribution each. Assuming an increase of uncertainty with depth, standard deviations for the shared distributions are increased for deeper formations. Furthermore, uncertainty regarding the magnitude of fault offset is incorporated by adding a skew normal probability distribution that is shared by all layer interface points in the hanging wall. A left skewed normal distribution is chosen to reflect the nature of throw on a normal fault, in particular the slip motion of the hanging wall block. Mainly negative values are returned by this distribution. This way, the offset nature of the normal fault is maintained and inversion to a reverse fault is avoided.

2.3 The value of interest for decision making

We define the trap volume V_t as the central feature of economic interest. For conducting straightforward volumetric calculations, we assume that found closed traps are always filled to spill, i.e. we only consider structural features as controlling mechanisms. This value is of central importance for calculating original oil or gas in place (OOIP/OOIG) and consequently, recoverable reserves. This type of estimation is also the only approach to assess the amount of hydrocarbons in a reservoir before production has started (Dean, 2007; Morton-Thompson et al., 1993).

By declaring these connections, we have given our model an economic significance. We can assume that the hydrocarbon trap volume is directly linked to project development decisions, i.e. investment and allocation of resources is represented by bidding on a volume estimate.

In the course of this work, we developed a set of algorithms to enable the automatic recognition and calculation of trap volumes in geological models computed by GemPy. The volume is determined on a voxel-counted basis via four conditions illustrated in Fig. 2 and further explained in Appendix A.

Following these conditions, we can define four major mechanisms which control the maximum trap volume: (1) the anticlinal spill point of the seal cap, (2) the cross-fault leak point at a juxtaposition of the reservoir formation with itself, (3) leakage due to juxtaposition with overlying layers and SSF failure, and (4) stratigraphical breach of the seal, when its voxels are not continuously connected above the trap. Due to the nature of our model, (3) and (4) will always result in complete trap failure.

Solid Earth Discuss., https://doi.org/10.5194/se-2019-57
Manuscript under review for journal Solid Earth
Discussion started: 27 March 2019

The trap volume V_t is a result from GemPy's implicit geological model computation. It is an output parameter dependent on deterministic and stochastic input parameters. With every model realization, input uncertainties will respectively propagate to the volume, which in turn is uncertain. We can thereby evaluate it using probabilistic methods and Bayesian decision theory in particular, as explained in the following.

2.4 Bayesian decision theory

We view the statistical analysis of our model from a Bayesian perspective, which is most importantly characterized by its preservation of uncertainty. Its principles have been presented and discussed extensively in literature (see Jaynes (2003), Box and Tiao (2011), Harney (2013), Gelman et al. (2014) and Davidson-Pilon (2015)). The Bayesian approach is widely seen as intuitive and inherent in the natural human perspective. It regards probability as a measure of belief about a true state of nature. Such beliefs can be assigned to individuals. Thus, different and even contradicting beliefs about a true state of nature might be held by different individuals, based on variations and disparities in the information available to each one individual.

In this work, the decision problem is one of estimating the true state of our value of interest, which we denote θ. Estimations are based on probability distributions attained from: (1) simple Monte Carlo error propagation, and (2) Bayesian inference using Markov chain Monte Carlo simulation. For (1), we are dealing with a prior probability distribution $p(\theta)$ that results from the deterministic function of the uncertain model input parameters. For (2), the prior distribution is revalued using Bayesian inference (see Appendix B) given the presence of additional statistical information y, and using likelihood functions $p(y|\theta)$. Decision making is then based on the resulting posterior probability $p(\theta|y)$. In general, Bayesian inference is about updating a belief and reaching an estimate that is less wrong.

2.4.1 Likelihoods

For the application of Bayesian inference, we implement two types of likelihoods:

1. **Layer thickness likelihoods:** With every model realization, we extract the z-distance between layer boundary input points at a central $x - y$ position (x = 1100 m, y = 1000 m) in our input interpolation data. Resulting thicknesses can then be passed on to stochastic functions in which we define thickness likelihoods via normal distributions.

2. **SSF likelihood**: SSF values are realized over more complex parameter compositions. We base this likelihood on a normal distribution which we link to the geological model output.

The inclusion of these likelihood is based on purely hypothetical assumptions and is intended to provide the opportunity to explore the effects different types and scenarios of additional information might have. While the thickness likelihood functions are dependent on input parameters directly, the implementation of the SSF likelihood function requires a full computation of the model and extended algorithms of structural analysis.

Solid Earth Discuss., https://doi.org/10.5194/se-2019-57
Manuscript under review for journal Solid Earth
Discussion started: 27 March 2019

2.4.2 Loss, expected loss and loss functions

Common point estimates, such as the mean and the median of a distribution, usually come with a measure for their accuracy (Berger, 2013). However, it has been argued by Davidson-Pilon (2015) that by using pure accuracy metrics, while this technique is objective, it ignores the original intention of conducting the statistical inference in cases, in which payoffs of decisions are valued more than their accuracies. A more appropriate approach can be seen in the use of loss functions (Davidson-Pilon, 2015).

Loss is a statistical measure of how "bad" an estimate is. Estimate-based decision are also referred to as actions a. Loss is defined as $L(\theta, a)$, so $L(\theta_1, a_1)$ is the actual loss incurred when action a_1 is taken while the true state of nature is θ_1 (Berger, 2013). The magnitude of incurred loss related to an estimate is defined by a loss function, which is a function of the estimate and the true value of the parameter (Wald, 1950; Davidson-Pilon, 2015):

$$L(\theta, \hat{\theta}) = f(\theta, \hat{\theta}). \tag{1}$$

So, how "bad" a current estimate is, depends on the way a loss function weights accuracy errors and returns respective losses. Two standard loss functions are the absolute-error and the squared-error loss function. Both are objective, symmetric, simple to understand and commonly used

Davidson-Pilon (2015) and Hennig and Kutlukaya (2007) have proposed that it might be useful to move on from standard objective loss functions to the design of customized loss functions that specifically reflect an individual's (i.e. the decision maker's) objectives, preferences and outcomes. Hennig and Kutlukaya (2007) argue that choosing and designing a loss function involves the translation of informal aims and interests into mathematical terms. This process naturally implies the integration of subjective decisions and subjective elements. According to them, this is not necessarily unfavorable or less objective, as it may better reflect an expert's perspective on the situation.

Standard symmetric loss functions can easily be adapted to be asymmetric, for example by weighting errors on the negative side stronger than those on the positive side. Preference over estimates larger than the true value (i.e. overestimation) is thus incorporated in an uncomplicated way.. Much more complicated designs of loss functions are possible, depending on purpose, objective and application.

The presence of uncertainty during decision making implies that the true parameter value is unknown and thus the truly incurred loss $L(\theta, a)$ cannot be known at the time of making the decision. The Bayesian perspective considers unknown parameters as random variables and samples that are drawn from the posterior distribution as possible realizations of the unknown parameter, i.e. all possible true values are represented by this distribution.

Given a posterior distribution $p(\theta|y)$, the expected loss of choosing an estimate $\hat{\theta}$ over the true parameter θ (after evidence y has been observed) is defined by (Davidson-Pilon, 2015):

$$l(\hat{\theta}) = E_\theta[L(\theta, \hat{\theta})]. \tag{2}$$

The expectation symbol E is subscripted with θ, by which it is indicated that θ is the respective unknown variable. This expected loss l is also referred to as the Bayes risk of estimate $\hat{\theta}$ (Berger, 2013; Davidson-Pilon, 2015).

Solid Earth Discuss., https://doi.org/10.5194/se-2019-57
Manuscript under review for journal Solid Earth
Discussion started: 27 March 2019

By the Law of Large Numbers, the expected loss of $\hat{\theta}$ can be approximated drawing a large sample size N from the posterior distribution, respectively applying a loss function L and averaging over the number of samples (Davidson-Pilon, 2015):

$$\frac{1}{N}\sum_{i=1}^{N} L(\theta_i, \hat{\theta}) \approx E_\theta[L(\theta, \hat{\theta})] = l(\hat{\theta}). \tag{3}$$

Minimization of a loss function returns a point estimate known as Bayes action or Bayesian estimator, which is the decision with the least expected loss according to the loss function, and the decision we are interested in in this work (Berger, 2013; Moyé, 2006).

2.5 Customization of our case-specific loss function

Assigning an economic notion to our model and assuming the case of an actor or decision maker in any field naturally necessitates the consideration of preferences, interests and the overall subjective perspective such an individual or for example a company might have. Further constraints and conditions can also be specific to the field, industry or generally to the problem at hand. Consequently, the design of a more specific non-standard and possibly asymmetric loss function might be required. One that includes subjective aspects and difference in weighting of particular risks, arising from an actor's inherent preferences and the environment in which the actor has to make a decision. In the face of several uncertain parameters, a perfectly true estimate is virtually unattainable. However, an attempt can be made to design a custom loss function that returns a Bayesian estimator involving the least bad consequences for an individual in a specific environment (Davidson-Pilon, 2015; Hennig and Kutlukaya, 2007).

For our example case of trap volume estimation, we develop a custom loss function in five steps. Ideally, an actor would like to know the exact trap volume, so that resources can be allocated appropriately in order to acquire economic gains. This conscious and irrevocable allocation is the decision to be made or action to be taken (Bratvold and Begg, 2010). Thus, we treat estimating as equivalent to making a decision. Deviations from the unknown true value in the form of over- and underestimation bring about an error and loss accordingly. In steps I - IV we make assumptions about the significance of such deviations and how they differently contribute to risks in the general decision making environment.

It can be assumed that several actors in one such environment or sector may have the same general loss function but different affinities concerning the risks. This might be based for example on different psychological factors or economic philosophies followed by companies. It might also be based on budgets and options such actors have available. An intuitive example is the comparison of a small and a large company. A certain false estimate or error might have a significantly stronger impact on a company which has a generally lower market share and only few projects, than on a larger company which might possess a higher financial flexibility and for which one project is only one of many development options in a portfolio. We therefore introduce the concept of varying risk affinities in the final step V.

- **Step I - Choosing a standard loss function as starting point**: In our case, we assume that investments increase linearly with linear growth in the value of the resource (i.e. the volume). For this reason, we choose the symmetric absolute-error

Solid Earth Discuss., https://doi.org/10.5194/se-2019-57
Manuscript under review for journal Solid Earth
Discussion started: 27 March 2019

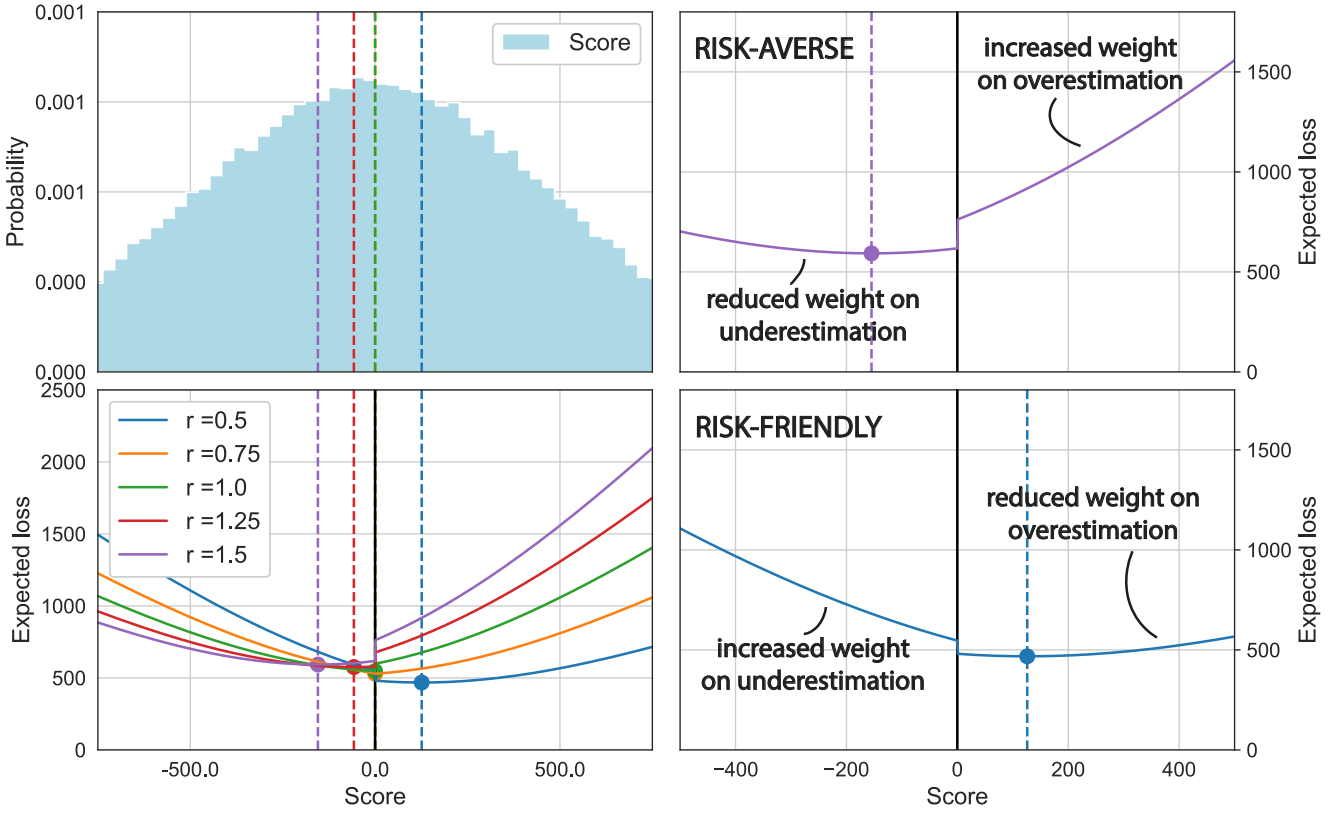

Figure 3. Plotting of expected loss realizations after including the risk affinity factor r in the loss function (see Eq. 8) for actors with risk affinities ranging from risk-friendly (r = 0.5 and 0.75), over risk-neutral (r = 1), to risk-averse (r = 1.25 and r = 1.5). Dots mark the respective positions of minimizing actions. We applied the function to samples from a normal distribution ($\mu = 0$, $\sigma = 500$) that represents the probability of a hypothetical score which is to be estimated. Jumps at zero are caused by the implementation of fatal over- and underestimation. Taking a closer look at the realizations for $r = 1.5$ and $r = 0.5$, we can recognize how they expect different losses and come to a different optimal decision given the same information. As in this case, positive and negative score values are equally likely, and overestimation errors are weighted stronger, only the most risk-friendly actor will bid on a positive estimate. Also, expected losses are lower for more risk-friendly decision makers.

Solid Earth Discuss., https://doi.org/10.5194/se-2019-57
Manuscript under review for journal Solid Earth
Discussion started: 27 March 2019

loss function as a basis for further customization steps:

$$L(\theta,\hat{\theta}) = |\theta - \hat{\theta}|. \tag{4}$$

– **Step II - Simple overestimation**: Considering the development of a hydrocarbon reservoir, it can be assumed that over-investing is worse than under-investing. Overestimating the size of an accumulation might for example lead to the installation of equipment or facilites that are actually redundant or unnecessary. This would come with additional unrecoverable expenditures. Consequences from underestimating ($0 < \hat{\theta} < \theta$), however, may presumably be easier to resolve. Additional equipment can often be installed later on. Hence, simple overestimation ($0 < \theta < \hat{\theta}$) is weighted stronger in this loss function by multiplying the error with an overestimation factor a:

$$L(\theta,\hat{\theta}) = |(\theta - \hat{\theta})|\ a. \tag{5}$$

– **Step III - Fatal overestimation**: The worst case for any project would be that its development is set into motion, expecting a gain, only to discover later that the value in the reservoir does not cover the costs of realizing the project, resulting in an overall loss. A petroleum system might also turn out to be a complete failure, containing no value at all, although the actor's estimate indicated the opposite. Here, we refer to this as fatal overestimation. A positive value is estimated, but the true value is zero or negative ($\theta \leq 0 < \hat{\theta}$). This is worse than simple overestimation, where both values are positive and a net gain is still achieved, which is only smaller then the best possible gain of expecting the true value. Fatal overestimation is included in the loss function by using another weighting factor b that replaces a:

$$L(\theta,\hat{\theta}) = |(\theta - \hat{\theta})|\ b. \tag{6}$$

In other words: With $b = 2$, fatal overestimation is twice as bad as simple underestimation.

– **Step IV - Fatal underestimation**: We also derive fatal underestimation from the idea of estimating zero (or a negative value), when the true value is actually positive ($\hat{\theta} \leq 0 < \theta$). This is assumed to be worse than simple overestimation, but clearly better than fatal overestimation. No already owned resources are wasted, it is only the potential value that is lost, i.e. opportunity costs that arise from completely discarding a profitable project. Fatal underestimation is weighted using a third factor c:

$$L(\theta,\hat{\theta}) = |(\theta - \hat{\theta})|\ c. \tag{7}$$

– **Step V - Including different risk affinities**: We now further adapt the loss function to consider varying risk affinities of different actors. We follow the approach of Davidson-Pilon (2015), who implemented different risk affinities by simply introducing a variable risk factor. Using different values for this factor, we can represented how comfortable an individual is with being wrong and furthermore which "side of wrong" is preferred by that decision maker (Davidson-Pilon, 2015). In our case, bidding lower is considered the cautious, risk-averse option, as smaller losses can be expected from underestimating. Guessing higher is deemed riskier, as losses from overestimation are greater. However, bidding

Solid Earth Discuss., https://doi.org/10.5194/se-2019-57
Manuscript under review for journal Solid Earth
Discussion started: 27 March 2019

correctly on a higher value, will also return a greater gain. It is assumed that risk-friendly actors care less about fatal underestimation, i.e. they will rather develop a project than discard it. In our finalized loss function, we simply include these considerations via a risk affinity factor r which alters the incurred losses respectively:

$$L(\theta,\hat{\theta}) = \begin{cases} |\theta-\hat{\theta}|\, r^{-0.5}, & \text{for } 0 < \hat{\theta} < \theta \\ |\theta-\hat{\theta}|\, a\, r, & \text{for } 0 < \theta < \hat{\theta} \\ |\theta-\hat{\theta}|\, b\, r, & \text{for } \theta \leq 0 < \hat{\theta} \\ |\theta-\hat{\theta}|\, c\, r^{-0.5}, & \text{for } \hat{\theta} \leq 0 < \theta \end{cases}, \text{ with } a,b,c,r \in \mathbb{Q}. \tag{8}$$

It is important to note that the weighting factors *a, b* and *c* can take basically any numerical values but should be chosen in a way that they appropriately represent the framework conditions of the problem. Here, we assume that simple overestimation is 25% ($a = 1.25$), fatal overestimation 100% ($b = 2$) and fatal underestimation 50% ($c = 1.5$) worse than simple underestimation. An example plot of actual incurred losses via this loss function can be found in Appendix C

According to Eq. 8, the risk-neutral loss function is returned for $r = 1$, as no re-weighting takes place. For $r < 1$, the weight on overestimating (*a, b*) is reduced and increased for fatal underestimation (*c*), as well as normal underestimation. This represents a risk-friendlier actor that is willing to bid on a higher estimate to attain a greater gain. For $r > 1$, the overestimation weight (*a, b*) is increased in the loss function, underestimation and fatal underestimation weight (*c*) are decreased and respectively more risk-averse actors are prompted to bid on lower estimates. Since risk neutrality is expressed by $r = 1$, we consider values $0 < r < 2$ to be the most appropriate choices to represent both sides of risk affinity equally. Accordingly different loss function realizations are plotted in Fig. 3.

It has to be emphasized that this is just one possible proposal for loss function customization. There exists not one perfect design for such a case (Hennig and Kutlukaya, 2007). Slight to strong changes can already be implemented by simply varying the values of the weighting factors *a, b* and *c*. Fundamentally different loss functions can also be based on a significantly different mathematical structure. Loss functions are customized regarding the problem environment and according to the subjective needs and objectives of the decision maker (Davidson-Pilon, 2015; Hennig and Kutlukaya, 2007). Thus, they are mostly defined by the actor expressing his perspective. Changes in the individual's perception and attitude might lead to further customization needs at a future point in time, as was reported by Hennig and Kutlukaya (2007).

3 Results

We applied our custom loss function to various different volume probability distributions resulting from stochastic simulations. First, reference results were created using only priors and simple Monte Carlo error propagation (10,000 sampling iterations, Scenario 1). Then we devised several scenarios of additional information and included these via likelihoods and Bayesian inference. For this, 10,000 MCMC sampling steps were conducted, with an additional burn-in phase of 1000 iterations. The prior parameter uncertainties were chosen to be identical for all simulations (see Table 1). Results of convergence diagnostics can be found in Appendix E.

Solid Earth Discuss., https://doi.org/10.5194/se-2019-57
Manuscript under review for journal Solid Earth
Discussion started: 27 March 2019

Table 2. Normal distribution mean (μ) and standard deviations (σ) for the likelihoods implemented in the different scenarios.

	Seal thickness		Reservoir thickness		SSF	
	μ [m]	σ [m]	μ [m]	σ [m]	μ	σ
Scenario 1	-	-	-	-	-	-
Scenario 2a	300	30	-	-	-	-
Scenario 2b	50	30	-	-	-	-
Scenario 3a	350	30	-	-	-	-
Scenario 3b	300	30	300	30	-	-
Scenario 4a	-	-	-	-	5.1	0.3
Scenario 4b	300	30	-	-	2	0.3

We present the following information scenarios:

1. **Prior-only** model
2. Introducing **seal thickness likelihoods**
   (a) Likely thick seal
   (b) Likely thin seal
3. Introducing **reservoir thickness likelihoods**
   (a) Likely thick reservoir
   (b) Likely thick reservoir and thick seal
4. Introducing **SSF likelihoods**
   (a) SSF likely near its critical value
   (b) Likely reliable SSF and thick seal

The implemented likelihoods are listed in Table 2.

For the comparison of results, we consider in particular the following measures: (1) probability field visualization, (2) occurrence of trap control mechanisms, (3) resulting trap volume distributions, and (4) consequent realization of expected losses and related decisions.

3.1 Prior-only model (Scenario 1)

Probability field visualization illustrates well how the prior uncertainty is based on normal distributions (see Fig. D2). Trap control mechanisms are listed in Table D2. For this prior-only scenario, all four relevant mechanisms occurred. The dominant factor is the anticlinal spill point with a 51.5 % rate of occurrence. It is followed by cross-fault leakage to the reservoir (25 %)

Solid Earth Discuss., https://doi.org/10.5194/se-2019-57
Manuscript under review for journal Solid Earth
Discussion started: 27 March 2019

and other permeable formations (12 %). Stratigraphical breaches of the seal were registered to be decisive in about 11 % of iterations. In only 0.5 % of iterations, the algorithm failed to recognize a mechanism, i.e. correct model realization failed.

Maximum trap volumes were calculated for each model iteration and plotted as a probability distribution in Fig. 4. In general, a wide range of volumes is possible, from zero to more than 3 million m^3. However, we can recognize a bimodal tendency: Low but positive volumes are less probable than significantly high volumes or complete failure ($V_t = 0$).

Consequently, applying our custom loss function to this distribution resulted in widely separated minimizing estimators for the differently risk-affine actors (see Fig. 4). Only the risk-friendliest estimates are found within the described highly positive mode of the distribution. Risk-averse individuals bid on significantly lower estimates or even zero. The risk-neutral decision is found between both modes and presents the highest expected loss. Expected losses decrease towards the extreme decisions and closer to the modes.

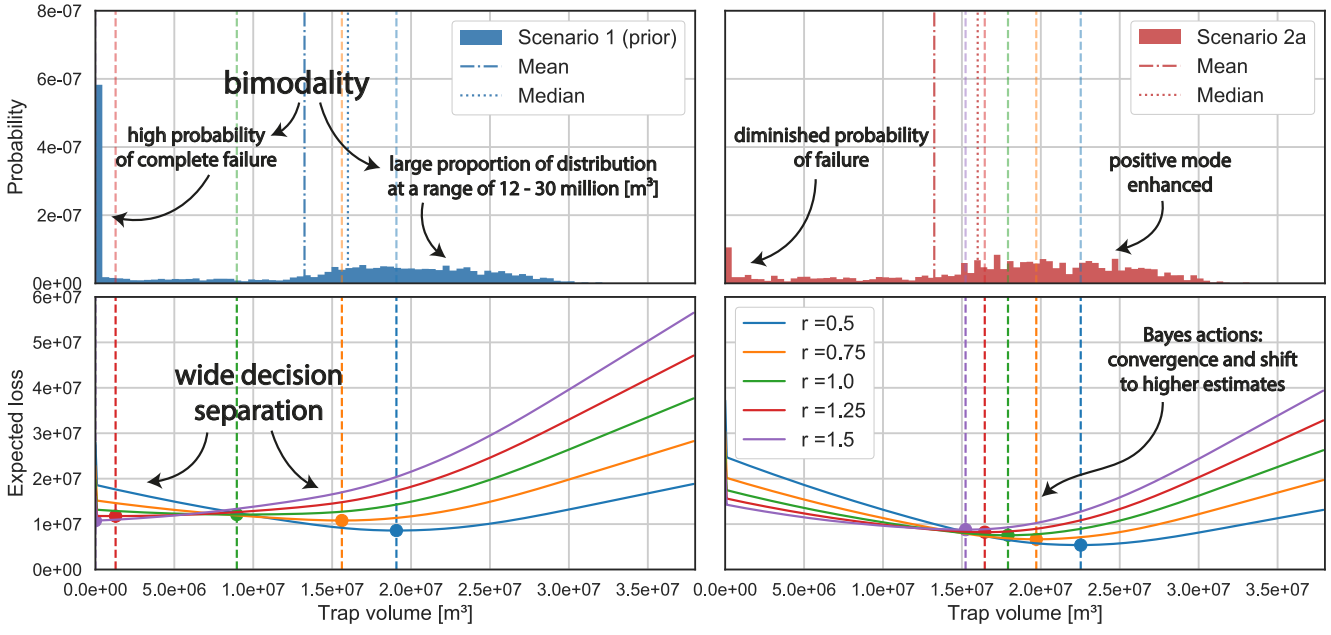

Figure 4. Trap volume distribution and resulting loss function realizations for Scenario 1 (prior) and Scenario 2a, where we introduced the likelihood of a thick seal. Comparing both, we can observe how the additional information reduced the bimodality in the posterior distribution (2a), particularly by reducing the probability of complete failure and enhancing positive probabilities. Consequently, Bayes actions converged and expected losses were reduced.

3.2 Introducing seal thickness likelihoods (Scenarios 2a and 2b)

We considered two scenarios of thickness likelihoods: The seal being (Scenario 2a) likely very thick, or (Scenario 2b) likely very thin (see Table 2).

Solid Earth Discuss., https://doi.org/10.5194/se-2019-57
Manuscript under review for journal Solid Earth
Discussion started: 27 March 2019

In Scenario 2a, probability visualization illustrates that the presence of a thick seal is very probable (see Fig. D2). For Scenario 2b, the presence of a reliable seal is questionable.

A high likelihood of a reliable seal cap (2a) significantly reduced the probability of trap failure, while enhancing the mode of highly positive outcomes (see Fig. 4). This coincides with the predominance of the anticlinal spill point (63 %) and the leak point to the same reservoir (36%) as control mechanisms. The occurrence of other mechanisms was negligible (see Table D2). Inversely, a likely thin seal (2b) virtually eliminated the positive mode and focused almost the whole distribution on complete failure. Accordingly, seal-breach related control mechanisms gained importance (65.5 % occurrence rate for stratigraphical seal breach).

In both scenarios, Bayes actions shifted towards the respectively emphasized modes. This came with overall convergence of decisions and reduction of expected losses. In Scenario 2a, all decision makers bid on a positive outcome. Risk-averse individuals experienced the strongest shift, but also present the highest expected losses. In Scenario 2b, all individuals decide to not allocate resources. Even the risk-friendliest actor moved to a zero estimate, where the most risk-averse bid had already been placed in the prior Scenario 1. However, although all decision coincide, expected losses increase from risk-averse to risk-friendly (see Table D1).

3.3 Introducing reservoir thickness likelihoods (Scenarios 3a and 3b)

We also tested scenarios for a likelihoods of a thick reservoir formation alone (Scenario 3a) and in combination with the likelihood of a thick seal (Scenario 3b; see Table 2. The overall effect of using these reservoir-based likelihoods turned out to be minor compared to the seal-related scenarios.

In Scenario 3a, failure probabilities slightly increased, resulting in a decision shift towards lower values (see Fig. D1). Results for Scenario 3b are very similar to those of 2b, as can also be seen in Table D1. There was no significant reduction of expected losses or shift in decisions by adding the likelihood of a thick reservoir to the likelihood of a thick seal.

3.4 Introducing SSF likelihoods

We considered two SSF-related likelihood scenarios. In Scenario 4a, we implemented solely a SSF likelihood that was based on a narrow normal distribution (μ = 5.1, σ = 0.3) with a mean near the critical value SSF_c = 5. In Scenario 4b, we combined the likelihood of a thick seal (2a) with a likely moderate but reliable SSF value (SSF normal distribution with mu = 2 and σ = 0.3). Figure 5 illustrates the posterior situations well.

Scenario 4a resulted in increased bimodality of the posterior distribution (see Fig. 6). Accordingly, the Bayes action divergence and expected losses increased. Only two trap control mechanisms remained relevant for 4a (see Table D2): anticlinal spill (66 %) and cross-fault leakage to overlying formations (34 %).

The results for 4b were comparable to those of 2a, but more pronounced. Entropies, particularly related to the seal thickness, were clearly reduced, also in the hanging wall. Probabilities of failure and low volumes were almost eliminated, further enhancing the highly positive mode. This consequently resulted in an even higher convergence of Bayes actions, as well as

Solid Earth Discuss., https://doi.org/10.5194/se-2019-57
Manuscript under review for journal Solid Earth
Discussion started: 27 March 2019

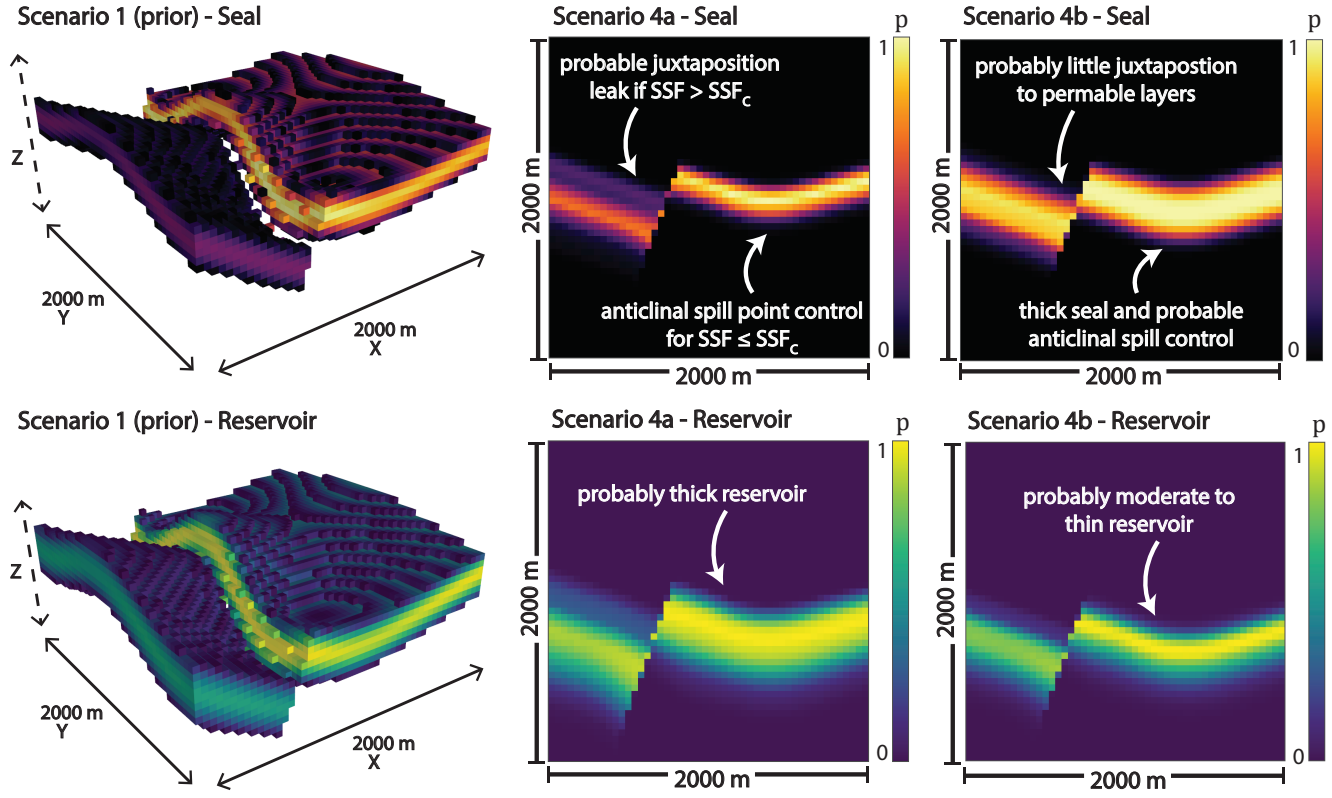

Figure 5. Probability field visualizations for seal and reservoir units in Scenarios 1 (prior), 4a and 4b. For Scenario 1, we used 3-D voxel visualizations and set a threshold at a probability of 0.5 (only voxels with a probability higher than 0.5 are shown). It can be recognized, that the seal is disrupted across the fault in more than 50 % of the prior model realizations. For the other scenarios, we show the full probability field for both units on a section through the middle of the model (y = 500 m), parallel to the $x - z$ plane.

reduction of expected losses compared to Scenario 2a. Anticlinal spill is the decisive control mechanism in 79.5 % of cases, otherwise only cross-fault leakage to the reservoir occurred (20.5 %).

4 Discussion

In this work, we build upon the recent advances presented by de la Varga et al. (2019) which enable us to view geological modeling as a probabilistic statistical problem. We expand on this by proposing custom loss functions as a useful decision-making tool when dealing with uncertain structural geological settings and to measure the effects of adding new information to a model. This is also aimed to illustrate the significance of the Bayesian perspective with regards to model interpretation in an economic context. As an explanatory example, we chose the hydrocarbon sector. This field is characterized by the necessity to make decisions in the face of high risks and potentially high rewards. These decisions are often closely linked to geological modeling and the estimation of reservoir-related values. By developing case-specific custom loss functions, we

Solid Earth Discuss., https://doi.org/10.5194/se-2019-57
Manuscript under review for journal Solid Earth
Discussion started: 27 March 2019

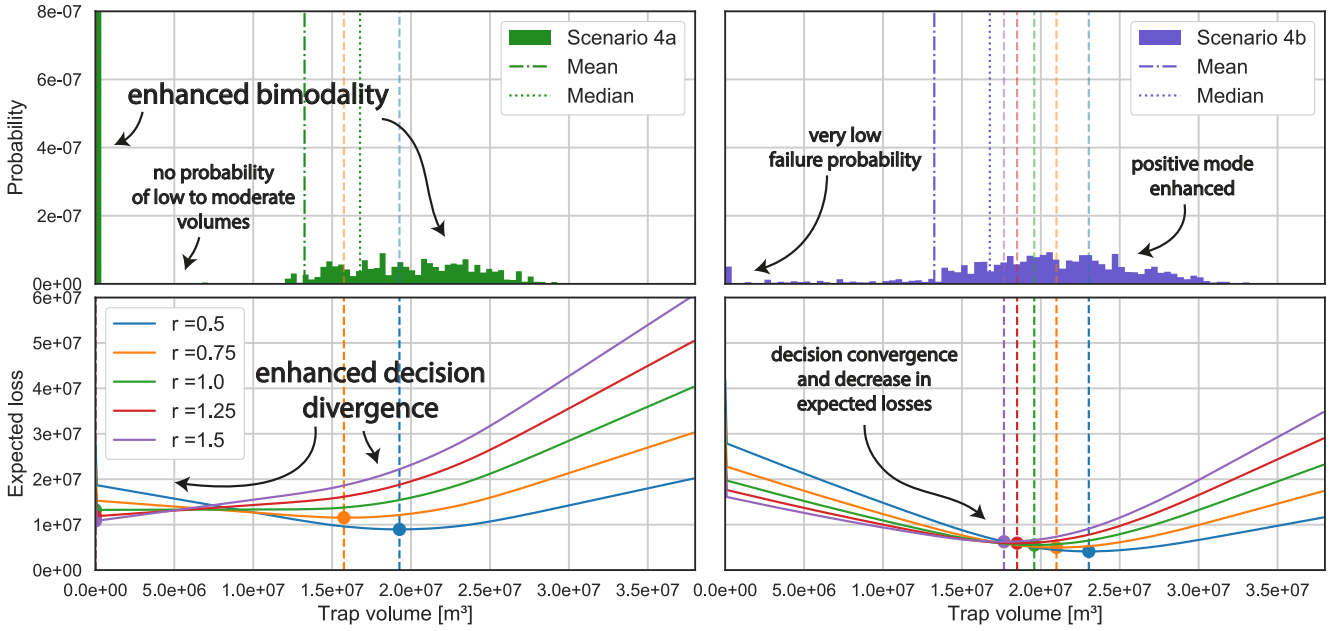

Figure 6. Trap volume distribution and resulting loss function realizations for Scenario 4a and Scenario 4b. Adding a likelihood of the SSF being around its critical value led to increased bimodality and an elimination of low to moderate volume probabilities. Bayes actions diverged accordingly in Scenario 4a. Implementing a reliable SSF value likelihood ($\mu = 2$, $\sigma = 0.3$) in combination with the thick seal likelihood from Scenario 2a, resulted in a emphasis on highly positive volumes. This, in turn, led to a stark convergence of decisions and reduction of expected losses.

intended to show that this estimation approach is suitable and useful to express the nature of complexities behind decision-making problems, decision environments and the risk-related behavior of actors.

4.1 State of knowledge, decision uncertainty and consequent decision making

As we defined trap volume to be in essence a deterministic function of uncertain model input parameters, uncertainties propagate to this parameter of interest when conducting stochastic simulations. We consider the resulting volume probability distributions to be expressions of the respective state of knowledge (or information) on which the decision making is to be based. As this should include all parameters and conditions relevant for decision making, we furthermore propose that the overall uncertainty inherent in this probability distribution can be referred to as "decision uncertainty" and that this entity should be viewed separately from geological model uncertainty.

By viewing decision making as a problem of optimizing a case-specific custom loss function applied to such a state of knowledge and decision uncertainty, we were able to observe clear differences in the respective behavior of distinctly risk-affine actors.

Solid Earth Discuss., https://doi.org/10.5194/se-2019-57
Manuscript under review for journal Solid Earth
Discussion started: 27 March 2019

The position and separation of their minimizing estimators, i.e. their decisions, manifested according to the properties of the value distributions. General spread and the occurrence of modes relative to the overall distribution and the relevant decision space appear to be particularly significant. High spread and bimodal tendencies, i.e. high overall uncertainty, resulted in a wider separation of different actions. Reduction of the distribution to one mode conversely led to their convergence. A decrease in decision uncertainty furthermore was accompanied by a reduction in expected loss for each Bayes estimator.

Considering these observations, we derive that the degree of action convergence and respective expected losses can be considered measures for the state of knowledge and decision uncertainty at the moment of making a decision. The better these are, the more similar the decisions of differently risk-affine actors and the lower their loss expectations are. Given perfect information all actors would bid on the same estimate (the true value) and expect no loss, since no risk would be present. It furthermore follows from this that the relevance of risk affinity decreases with greater reduction of decision uncertainty.

4.2 The impact of additional information on decision making

We used these loss-function-related indicators to assess the significance additional information might have for decision making. We observed that the impact on decision uncertainty, induced by Bayesian inference, is not simply strictly aligned with the change in uncertainty regarding model parameters, but on those parameter combinations which are relevant for the outcome of the value of interest. It seems to be of central importance (1) "where" in the model uncertainty is reduced, i.e. in which spatial area or regarding which model parameters, and (2) which possible outcome is enhanced in terms of probability. An increased probability of a thick or thin seal in our model equally reduced decision uncertainty significantly, by raising the probability of a positive or negative outcome, respectively. Improved certainty about our reservoir thickness, however, had far lesser impact on decision making. This shows that some areas and parameter combinations have a much greater influence on the decision uncertainty than others, depending on the way they contribute to the outcome of the value of interest.

Some types of additional information could even lead to increased decision uncertainty. We observed this in Scenario 4a. The introduced SSF likelihood practically constrained our geological model to two possible situations: (1) a trap which is sealed off from juxtaposing layers and full-to-spill, and (2) complete failure of the trap due to a breached seal across the fault. This made the decision problem a predominantly binary one and split the outcome distribution into two narrowed but distant modes. The resulting increase in decision divergence and expected losses show that, in some cases, adding information might leave actors in greater disagreement than before.

However, we furthermore have to consider that actors weight possible outcomes of the value distribution differently. They consequently are affected differently by the same type of information. Risk-friendly actors were the most robust in their decision making in the face of possible trap failure. Eliminating this risk proved to be far less significant to the most risk-friendly, than for risk-averse actors. Accordingly, it should be of foremost importance for risk-averse actors to reduce the uncertainty regarding critical factors, such as seal integrity, which might decide between the success and complete failure of a project. This is less relevant for risk-friendly decisions makers, who respectively might acquire a comparable benefit from knowing more about the probability of positive outcomes. They are less afraid of failure and than they are of missing out on opportunity.

Crucial risks might be easily assessed if they are dependent on only one or a few parameters, such as seal thickness. In other cases, they are derived from more complex parameter interrelations, as is the case for the Shale Smear Factor. To approach an effective mitigation of high risks, the complexities behind decisive factors need to be assessed thoroughly and respective parent parameters, as well as their interdependencies, need to be identified. This might enable a better understanding of which type of information is missing and where in the model additional data might be of use for improved decision making.

More of simply any type of information does not necessarily lead to better decisions. Instead, improved decision making is achieved by attaining the right kind of information that is able to shed light on uncertainties which are relevant to an individuals own goals and preferences, as well as the general problem at hand. Bratvold and Begg (2010) stated that value is not generated by uncertainty quantification or reduction in itself, but is created to the extent that these processes have potential to change a decision. Such decision changes were clearly indicated by the shifting of actions in our different scenarios. According to Hammitt and Shlyakhter (1999), the difference in expected payoff between the prior and posterior optimal decision gives the expected value of information. This raises the question as to what extend a change in expected losses in itself might be an indicator for the value of information and if there is value in gaining confidence in a decision, even though it remains unchanged.

4.2.1 The significance of our method for the hydrocarbon sector

While Monte Carlo simulation is by now common in the hydrocarbon sector, it does not make decisions, as Murtha et al. (1997) emphasized. It merely prepares for it. We believe that loss functions have the potential to go one step further. A hypothetical ideal loss function would consider all conditions in an economic environment, as well as perfectly represent preferences and goals of an actor and consequently be able to automatically find an optimal decision. While this is obviously unrealistic, we presume that an elaborate loss function might at least provide a very good preliminary decision recommendation. It might furthermore be able to weight risks that are not immediately apparent to an individual as a person. Furthermore, the influence of human biases and psychological behavioral challenges, as described by Bratvold and Begg (2010), could be mitigated.

Bayesian inference and MCMC methods have been applied for OOIP estimation and forecasting of reservoir productivity by Wadsley et al. (2005), Ma et al. (2006) and Liu et al. (2010). However, their research focused on history-matching simulations for already producing fields. Our approach of applying Bayesian inference for structural geological modeling and volumetric reservoir calculations is intended to support decision making in the earliest stages of a reservoir, when it has to be decided whether a project should be developed or not. Nevertheless, it was shown in the research conducted by Wadsley et al. (2005) that early volumetric OOIP estimates can be combined with later calculations from production data via MCMC methods.

Our continuous approach could be integrated into common discrete decision-making frameworks, such as decision trees. In real cases, normally only a limited number of options is given. In the context of hydrocarbon exploration and production, this would relate to fixed magnitudes of resource allocation, such as a certain number of required drilling wells or the size of a production platform. Based on such previously defined actual options, we could discretize our value probability distribution into sections, which represent each decision scenario accordingly. Our minimizing estimators would then indicate the best discrete option for a decision maker.

Solid Earth Discuss., https://doi.org/10.5194/se-2019-57
Manuscript under review for journal Solid Earth
Discussion started: 27 March 2019

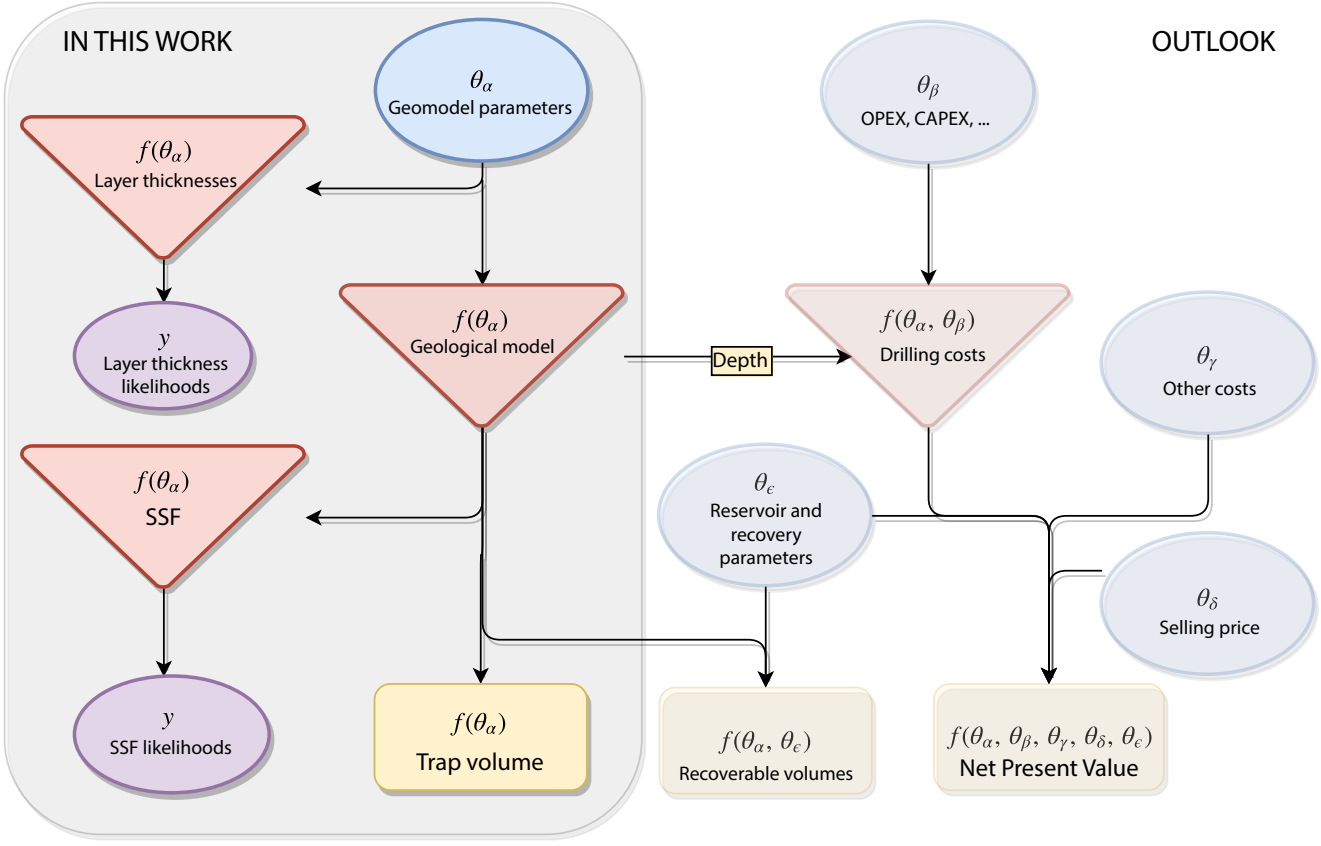

Figure 7. In this work, we applied our loss function approach to estimate a hydrocarbon trap volume. For this, we considered stochastic geomodeling parameters, defined deterministic functions to acquire volume, layer thicknesses and SSF values, and linked the latter two to respective likelihoods. Regarding the bigger picture, this methodology is expandable and could include other parameters and dependencies. By taking into account other reservoir parameters and recovery factors, we could for example base decision making on recoverable volumes. We could also take depth information from our model and combine this with other cost parameters to calculate drilling costs. Including additional costs, but also the selling price of hydrocarbons, we could attain the NPV as our final value of interest.

Solid Earth Discuss., https://doi.org/10.5194/se-2019-57
Manuscript under review for journal Solid Earth
Discussion started: 27 March 2019

4.2.2 Limitations and outlook

It has to be emphasized that we used a synthetic geological model, not based on real data. Nevertheless, it was designed to include some typical structural characteristics related to hydrocarbon systems. We developed algorithms aimed to consider the most common conditions that define structural traps. However, these conditions needed to be simplified and were implemented on a very conceptual level. Furthermore, uncertainties employed in the 3-D model related to z-positional values only and were thus of primarily one-dimensional nature. It follows that no effective uncertainty concerning the overall structural shape was implemented, particularly regarding anticlinal features and the lateral position of the spill point.

We defined risk affinity to be dependent on arbitrarily chosen risk factors which led to according reweighting. Davidson-Pilon (2015) used risk parameters determined by the maximal loss each actor could incur. Other approaches could be based on more tangible values, for example by making risk attitude dependent on a fixed budget.

There are still many points that could be expanded on in future research. It would be of interest to apply the same overall concept and methodology to an authentic case based on real datasets. Given a realistic economic scenario, including capital and operational expenditures of a project, possibly a full net-present-value (NPV) analysis could be conducted, applying a loss function to a NPV distribution (see Fig. 7). A more elaborate loss function could be customized on the base of surveys, acquiring the specific preferences of one or several companies and thus attaining a better profile of the economic environment, as well as the individuals acting in it.

Furthermore, additional and different uncertain parameters should be considered in the future. A respective next step regarding our model would be the incorporation of uncertainties which to a wider extent affect structural shapes in all three dimensions. Otherwise, non-structural reservoir parameters could be included as uncertain values, such as porosities and permeabilities of different layers. This might be of particular interest considering factors which are related to high risks in decision making.

We chose hydrocarbon systems and petroleum exploration as a sector for an exemplary application, but many other settings can be found in which geological modeling is of central significance for decision making. One example would be subsurface storage of fluids in a reservoir, such as carbon capture and storage (CCS). Questions regarding storage capacity and safety deal with similar conditions and geological problems as the ones presented this work. Other examples might be mining or geotechnical projects. In general, it does not lack of geo-related areas in which a good understanding of uncertainties, risks and the general state of information is crucial for good decision making, and in which custom loss functions could prove to be a beneficial tool.

Code and data availability. Code and model data used in this study are available in a GitHub repository found at http://github.com/cgre-aachen/loss_function_decision_making_paper (DOI: 10.5281/zenodo.2595357).

Solid Earth Discuss., https://doi.org/10.5194/se-2019-57
Manuscript under review for journal Solid Earth
Discussion started: 27 March 2019

Appendix A: Determination of the maximum trap volume

The volume is calculated on a voxel-count basis. To assign model voxels to the trap feature, it is checked whether the following conditions (illustrated in Figure 2) are satisfied by each individual voxel:

1. **Labeled as reservoir formation:** The voxel has been assigned to the target reservoir formation (see Sandstone 1 in Fig. 2 (1)) in GemPy's lithology block model.

2. **Location above spill point horizon:** The voxel is located vertically above the final spill point of the trap. In the algorithm to find this final spill point, it is distinguished between a spill point defined by the folding structure, referred to as anticlinal spill point, and a cross-fault leak point, that depends on the magnitude of displacement and the resulting nature of juxtapositions. Once both of these points have been determined, the higher one is defined to be the final spill point used to determine the maximum fill capacity of the trap. Given a juxtapostion with layers overlying the seal, due to fault displacement, the respective section is checked for fault sealing by taking into account the Shale Smear Factor (SSF) value which is the ratio of fault throw magnitude D to displaced shale thickness T (Lindsay et al., 1993; Yielding et al., 1997; Yielding, 2012):

   $$\mathrm{SSF} = \frac{D}{T}. \tag{A1}$$

   We attain both D and T by examining the contact between the seal lithology voxels and the fault surface.

   For our model, we define the critical SSF to be $\mathrm{SSF_c} = 5$. We assume that cross-fault sealing is breached when this threshold is surpassed. For simplicity, the fault is considered to be sealing along its plane.

3. **Location inside of closed system:** The voxel is part of a model section inside of the main anticlinal feature. All of the voxels inside this particular section are separated from the borders of the model by voxels that do not meet the first two conditions above, which primarily means that they are encapsulated by seal voxels upwards and laterally. This condition is relevant under the assumption, that connection to the borders of the model lead to leakage. A trap is thus defined as a closed system in this model and trap closure is assumed to be void outside of the space of information, i.e. the model space. In our example model, this also means that hydrocarbons escape in the hanging wall due to respective layer dipping upwards towards the model borders.

It has to be emphasized that these conditions have been fitted to our synthetic example model. For other models featuring different geological properties, structures and levels of complexities, these conditions and respective algorithms might not apply. Models of higher complexities will surely require the introduction of further conditions.

A1 Anticlinal spill point detection

Regarding anticlinal structures and traps, it can be observed that, geometrically and mathematically, a spill point is a saddle point of the reservoir top surface in 3-D. This was described by Collignon et al. (2015), who pointed out that the linkage of

Solid Earth Discuss., https://doi.org/10.5194/se-2019-57
Manuscript under review for journal Solid Earth
Discussion started: 27 March 2019

folds is given by saddle points. These are thus a controlling factor for spill-related migration from respective structural traps. For anticlinal traps, closure can consequently be defined as the distance between the saddle point (i.e. spill point) and maximal point of the trap (Collignon et al., 2015).

Regarding a surface defined by $f(x, y)$, a local maximum at (x_0, y_0, z_0) would resemble a hill top (Guichard et al., 2013). Local maxima will be found looking at the cross-sections in the planes $y = y_0$ and $x = x_0$. Furthermore, the respective partial derivatives (i.e. gradients) $\frac{\delta z}{\delta x}$ and $\frac{\delta z}{\delta y}$ will equal zero at x_0 and y_0, i.e. that the extremum is a stationary point (Guichard et al., 2013; Weisstein, 2017). In the context of a geological reservoir system, such a hill can be regarded as a representation of an anticlinal structural trap. Local minima are defined analogously, presenting local minima in both planes at a stationary point (Guichard et al., 2013). A saddle point, however, is a stationary point, while not being an extremum (Weisstein, 2017). In general, saddle points can be distinguished from extrema by applying the second derivative test (Guichard et al., 2013; Weisstein, 2017): Considering a 2D function $f(x, y)$ with continuous partial derivatives at a point (x_0, y_0), so that $f_x(x_0, y_0) = 0$ and $f_x(x_0, y_0) = 0$, the following discriminant D can be introduced:

$$D(x_0, y_0) = f_{xx}(x_0, y_0) f_{yy}(x_0, y_0) - f_{xy}(x_0, y_0)^2. \tag{A2}$$

Using this, the following holds for a point (x_0, y_0):

1. If $D > 0$ and $f_{xx}(x_0, y_0) < 0$, there is a local maximum.
2. If $D > 0$ and $f_{xx}(x_0, y_0) > 0$, there is a local minimum.
3. If $D < 0$, there is a saddle point at the point (x_0, y_0).
4. If $D = 0$, the test fails (Guichard et al., 2013).

According to Verschelde (2017), a saddle point in a matrix is maximal in its row and minimal in its column. This corresponds to the logical geometrical deduction, that a saddle point for a surface defined by $f(x, y)$ is marked by a local maximum in one plane, but a local minimum in the perpendicular plane. In our spill point detection algorithm, we make use of GemPy's ability to return layer boundary surfaces (simplices and vertices) as well as the gradients of the potential fields in discretized arrays:

1. We first look for vertices at which the surface of interest coincides with a gradient zero point.
2. Then, we check for the change in gradient sign at each such point in perpendicular directions. If they are opposite to one another, we can classify the vertex as a saddle point.
3. Lastly, we declare the highest saddle point to be our anticlinal spill point.

A2 Cross-fault leak point detection

For the potential point of leakage to formations underlying the seal across the normal fault (including the reservoir itself), we take the highest z-position of the reservoir units' contact (voxelized) with the fault in the hanging wall.

Solid Earth Discuss., https://doi.org/10.5194/se-2019-57
Manuscript under review for journal Solid Earth
Discussion started: 27 March 2019

In the case of a juxtaposition with seal-overlying formations and a failed SSF-check, the maximum contact of the trap with the fault becomes the final spill point. Due to the shape of the trap in our model, we can then expect full leakage and set the maximum trap volume to zero.

A3 Calculating the maximum trap volume

Have all trap voxels been determined via the conditions defined in Section 2.3, the maximum trap volume V_t is calculated by simply counting the number of trap voxels and rescaling their cumulative volume depending on the resolution in which the model was computed:

$$V_t = n_v * (\frac{S_o}{R_m})^3, \tag{A3}$$

Where n_v is the number of trap voxels, S_o gives the original scale and R_m the used resolution for the model.

For the example of a cubic geological model with an original extent of 2000 m in three directions, computed using a resolution of 50 voxels in every direction, the scale factor is 40 m. Every voxel thus accounts for $40\ \text{m} * 40\ \text{m} * 40\ \text{m} = 64,000\ \text{m}^3$ in volume. It has to be noted, that this direct approach to rescaling and calculating the volume requires the model to be computed in cubic voxels.

Appendix B: Bayesian inference

Bayesian inference is defined by and conducted via the following equation, called the Bayes' Theorem (Jaynes, 2003; Gelman et al., 2014; Box and Tiao, 2011; Harney, 2013; Davidson-Pilon, 2015):

$$p(\theta|y) = \frac{p(y|\theta)p(\theta)}{p(y)} \propto p(y|\theta)p(\theta). \tag{B1}$$

Appendix C: Further analysis of the custom loss function

For better understanding of how our custom loss function determines the incurrence of loss, actual losses for three fixed true values and risk-neutrality (r = 1) are plotted in Fig. C1.

Appendix D: Results data

Solid Earth Discuss., https://doi.org/10.5194/se-2019-57
Manuscript under review for journal Solid Earth
Discussion started: 27 March 2019

Table D1. Decision results for all considered scenarios and each actor. Respective optimal estimates (decisions) are represented by $\hat{\theta}$, while $\Delta\hat{\theta}$ indicates posterior changes relative to the prior (Scenario 1) result. Expected losses are given by l, changes relative to the prior by Δl.

		Decision makers				
		risk-friendly		**risk-neutral**		**risk-averse**
		r = 0.5	r = 0.75	r = 1.0	r = 1.25	r = 1.5
Scenario 1	$\hat{\theta}$	19072000.00	15616000.00	8960000.00	1280000.00	0.00
Prior	l	8582112.55	10785632.54	12100484.80	11759772.46	10763671.94
Scenario 2a	$\hat{\theta}$	22528000.00	19712000.00	17920000.00	16448000.00	15232000.00
Thick seal	$\Delta\hat{\theta}$	3456000.00	4096000.00	8960000.00	15168000.00	15232000.00
	l	5387582.96	6654239.73	7544384.00	8220155.30	8776678.80
	Δl	-3194529.59	-4131392.81	-4556100.80	-3539617.16	-1986993.14
Scenario 2b	$\hat{\theta}$	0.00	0.00	0.00	0.00	0.00
Thin seal	$\Delta\hat{\theta}$	-19072000.00	-15616000.00	-8960000.00	-1280000.00	0.00
	l	2743719.13	2240237.29	1940102.40	1735280.34	1584086.98
	Δl	-5838393.42	-8545395.25	-10160382.40	-10024492.12	-9179584.96
Scenario 3a	$\hat{\theta}$	17408000	8640000	0	0	0
Thick reservoir	$\Delta\hat{\theta}$	-1664000.00	-6976000.00	-8960000.00	-1280000.00	0.00
	l	10073515.53	12159993.48	11319609.6	10124566.62	9242422.54
	Δl	1491402.98	1374360.94	-780875.20	-1635205.84	-1521249.40
Scenario 3c	$\hat{\theta}$	22784000.00	20096000.00	18432000.00	16960000.00	15680000.00
Thick reservoir and seal	$\Delta\hat{\theta}$	3712000.00	4480000.00	9472000.00	15680000.00	15680000.00
	l	5380782.45	6658861.07	7551644.80	8278631.71	8857405.68
	Δl	-3201330.10	-4126771.47	-4548840.00	-3481140.75	-1906266.26
Scenario 4a	$\hat{\theta}$	19264000.00	15744000.00	0.00	0.00	0.00
Near critical SSF	$\Delta\hat{\theta}$	192000.00	128000.00	-8960000.00	-1280000.00	0.00
	l	8959284.13	11533073.67	13250828.80	11851901.58	10819256.41
	Δl	377171.58	747441.13	1150344.00	92129.12	55584.47
Scenario 4b	$\hat{\theta}$	23040000.00	20992000.00	19584000.00	18496000.00	17664000.00
Reliable SSF and thick seal	$\Delta\hat{\theta}$	3968000.00	5376000.00	10624000.00	17216000.00	17664000.00
	l	4112858.01	4964529.37	5513651.20	5929335.97	6245426.13
	Δl	-4469254.54	-5821103.17	-6586833.60	-5830436.49	-4518245.81

Solid Earth Discuss., https://doi.org/10.5194/se-2019-57
Manuscript under review for journal Solid Earth
Discussion started: 27 March 2019

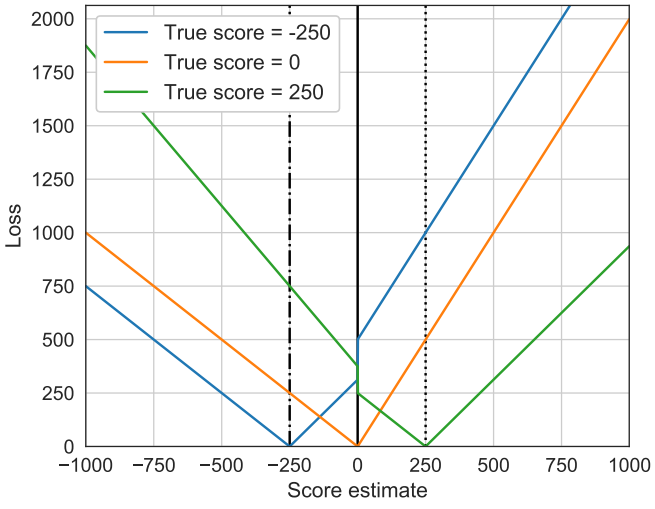

Figure C1. Loss based on the risk-neutral custom loss function (Eq. 8) for determined true scores of -250, 0 and 250. This plot is meant to clarify the way real losses are incurred for each guess, relative to a given true value. The expected loss, as seen in Fig. 3 is acquired by arithmetically averaging such deterministic loss realizations based on the true score probability distribution by using Eq. 3.

Solid Earth Discuss., https://doi.org/10.5194/se-2019-57
Manuscript under review for journal Solid Earth
Discussion started: 27 March 2019

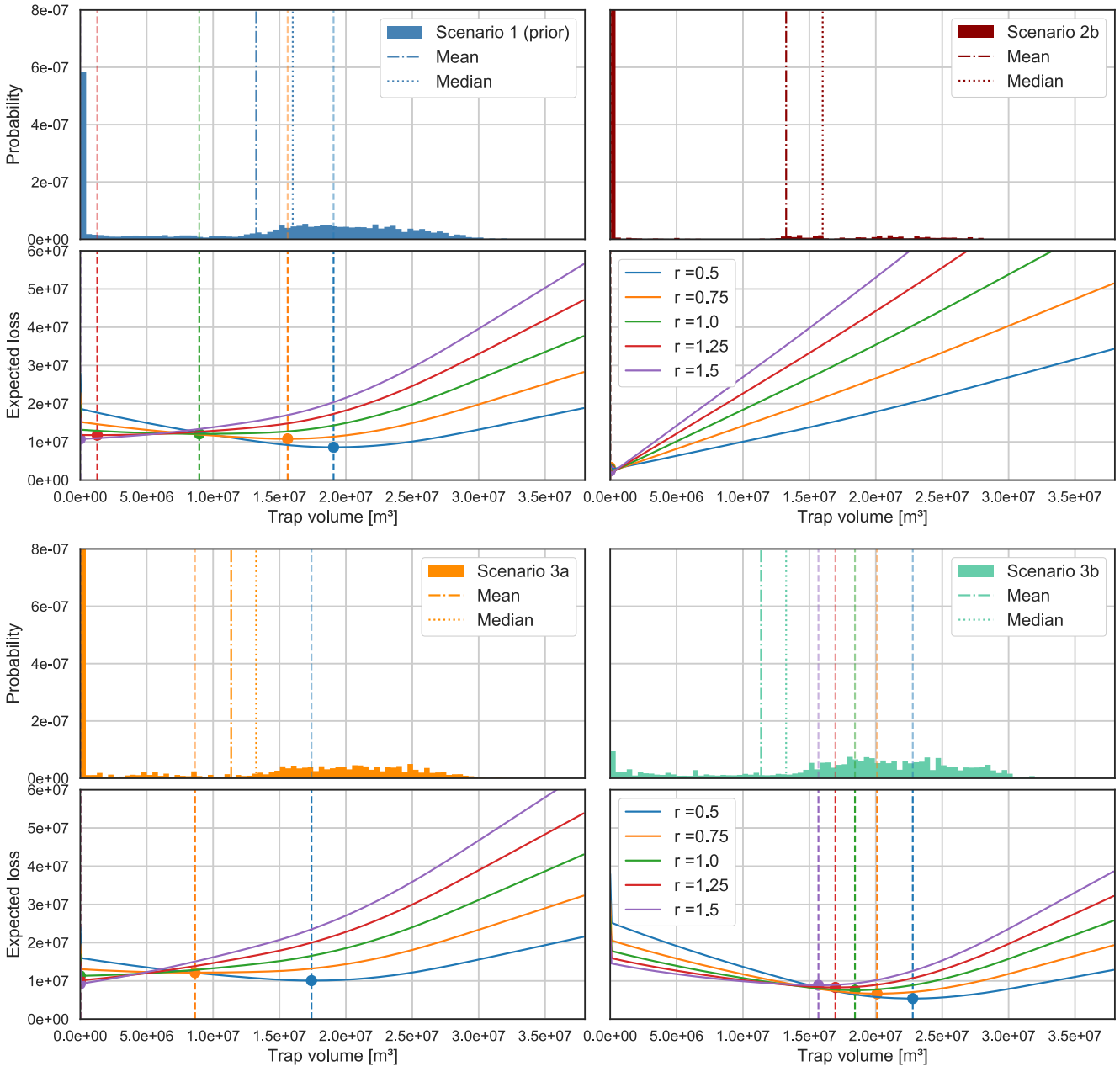

Figure D1. Posterior trap volume distributions and respective loss function realization plots for Scenarios 1 (prior), 2b, 3a and 3b.

Solid Earth Discuss., https://doi.org/10.5194/se-2019-57
Manuscript under review for journal Solid Earth
Discussion started: 27 March 2019

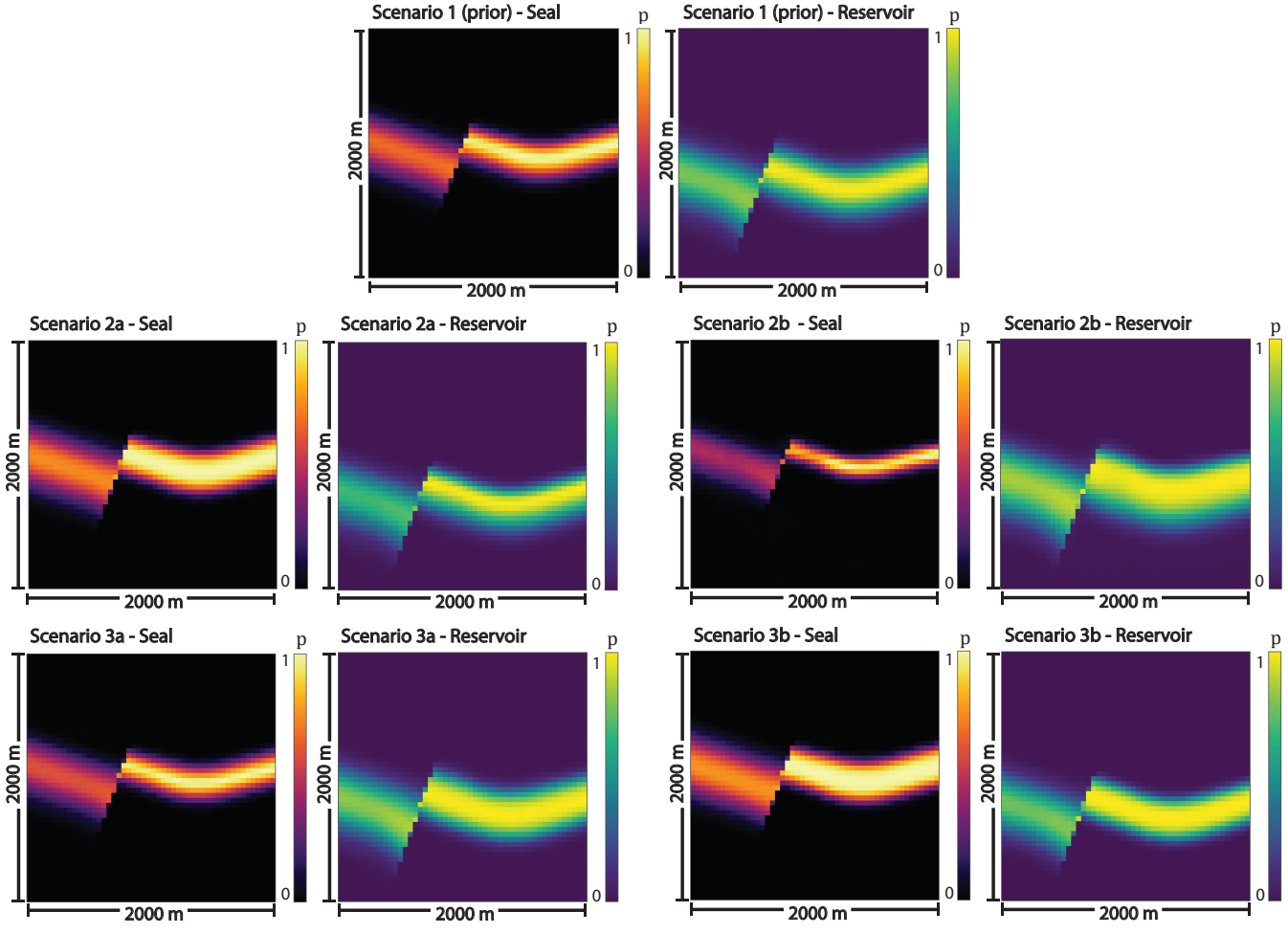

Figure D2. Probability field visualizations for Scenarios 1 to 3b.

Solid Earth Discuss., https://doi.org/10.5194/se-2019-57
Manuscript under review for journal Solid Earth
Discussion started: 27 March 2019

Table D2. Occurrence rate of trap control mechanisms in % for each information scenario.

	1 - Anticlinal spill	2 - Leak to reservoir	3 - Leak to overlying	4 - Stratigraphic breach	5 - Unclear
Scenario 1	51.47	25.11	12.36	10.56	0.5
Scenario 2a	63.1	35.8	0.41	0.49	0.2
Scenario 2b	10.04	1.53	20.82	65.51	2.1
Scenario 3a	41.99	23.21	23.06	11.38	0.36
Scenario 3b	61.86	36.59	0.53	1.02	0
Scenario 4a	66.4	0.01	33.59	0	0
Scenario 4b	79.45	20.55	0	0	0

Appendix E: MCMC convergence

Solid Earth Discuss., https://doi.org/10.5194/se-2019-57
Manuscript under review for journal Solid Earth
Discussion started: 27 March 2019

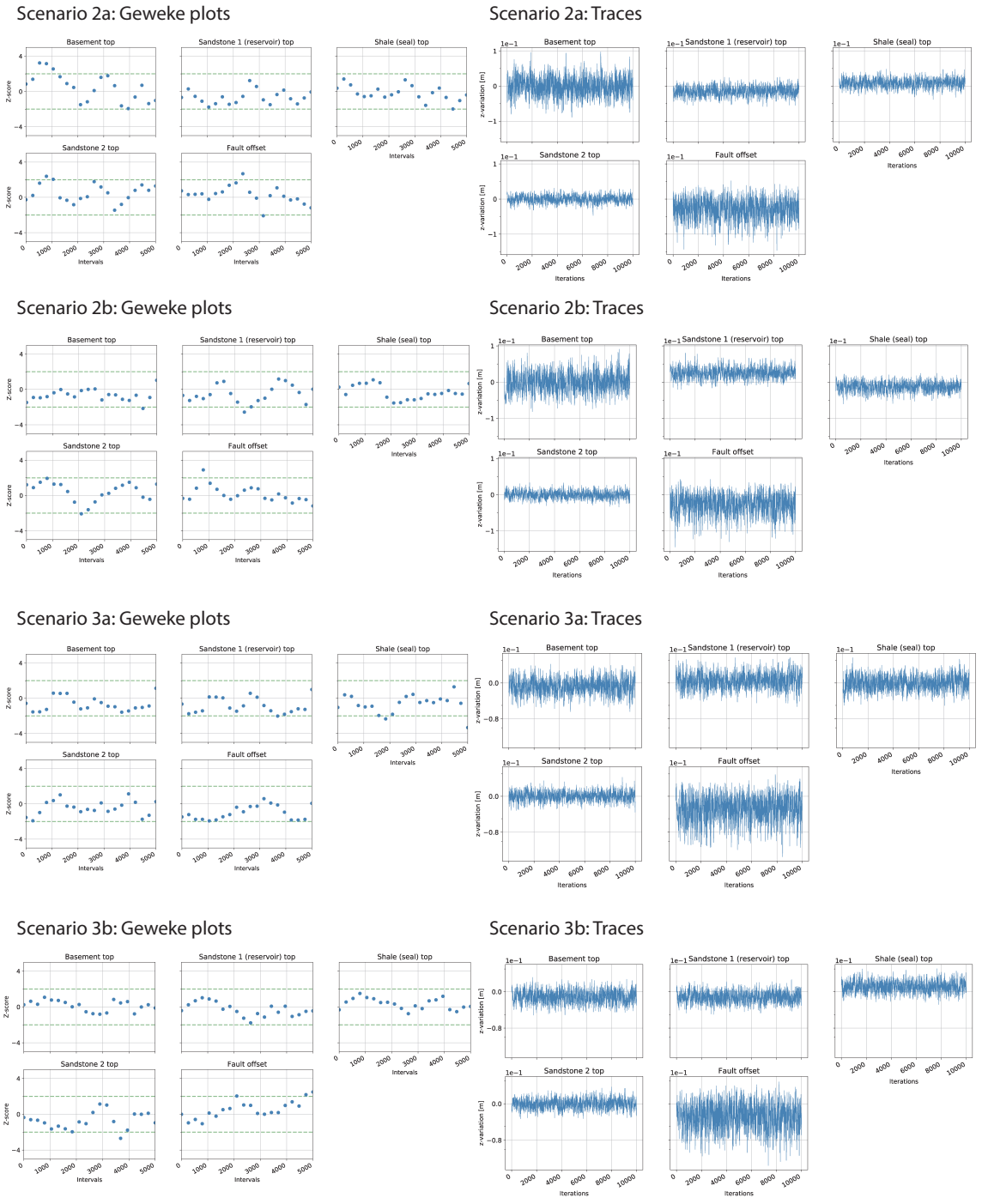

Figure E1. Geweke plots and traces for Scenarios 2a to 3b.

Solid Earth Discuss., https://doi.org/10.5194/se-2019-57
Manuscript under review for journal Solid Earth
Discussion started: 27 March 2019

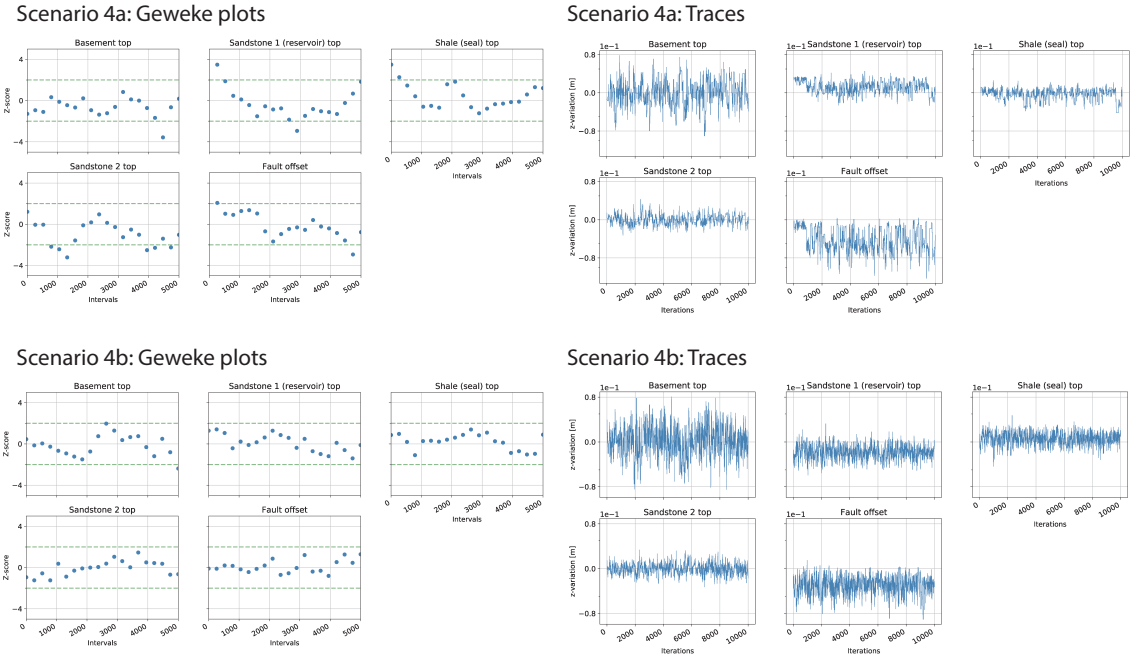

Figure E2. Geweke plots and traces for Scenarios 4a and 4b.

Solid Earth Discuss., https://doi.org/10.5194/se-2019-57
Manuscript under review for journal Solid Earth
Discussion started: 27 March 2019

Competing interests. The authors declare that they have no competing interests.

Acknowledgements. We would like to thank Cameron Davidson-Pilon for his comprehensive, free introduction into Bayesian methods which inspired parts of this research. Special thanks to Alexander Schaaf for helping with 3-D visualizations.

References

Bardossy, G. and Fodor, J.: Evaluation of Uncertainties and Risks in Geology: New Mathematical Approaches for their Handling, Springer, Berlin, Germany, 2004.

Berger, J. O.: Statistical decision theory and Bayesian analysis, Springer Science & Business Media, 2013.

Box, G. E. and Tiao, G. C.: Bayesian inference in statistical analysis, vol. 40, John Wiley & Sons, 2011.

Bratvold, R. and Begg, S.: Making good decisions, Society of Petroleum Engineers, 2010.

Caers, J.: Modeling Uncertainty in the Earth Sciences, John Wiley & Sons, Ltd, Chichester, UK, 2011.

Calcagno, P., Chilès, J.-P., Courrioux, G., and Guillen, A.: Geological modelling from field data and geological knowledge: Part I. Modelling method coupling 3D potential-field interpolation and geological rules, Physics of the Earth and Planetary Interiors, 171, 147–157, 2008.

Chatfield, C.: Model Uncertainty, Data Mining and Statistical Inference, Journal of the Royal Statistical Society. Series A (Statistics in Society), 158, 419–466, 1995.

Collignon, M., Fernandez, N., and Kaus, B.: Influence of surface processes and initial topography on lateral fold growth and fold linkage mode, Tectonics, 34, 1622–1645, 2015.

Davidson-Pilon, C.: Bayesian Methods for Hackers: Probabilistic Programming and Bayesian Inference, 2015.

de la Varga, M. and Wellmann, J. F.: Structural geologic modeling as an inference problem: A Bayesian perspective, Interpretation, 4, SM1–SM16, 2016.

de la Varga, M., Schaaf, A., and Wellmann, F.: GemPy 1.0: open-source stochastic geological modeling and inversion, Geoscientific Model Development, 12, 1–32, https://doi.org/10.5194/gmd-12-1-2019, https://www.geosci-model-dev.net/12/1/2019/, 2019.

Dean, L.: Reservoir Engineering for Geologists - Volumetric Estimation, The Monthly Magazine of the Canadian Society of Petroleum Geologists, pp. 11–14, 2007.

Gelman, A., Carlin, J. B., Stern, H. S., and Rubin, D. B.: Bayesian data analysis, vol. 2, Taylor & Francis, 2014.

Geweke, J. et al.: Evaluating the accuracy of sampling-based approaches to the calculation of posterior moments, vol. 196, Federal Reserve Bank of Minneapolis, Research Department Minneapolis, MN, USA, 1991.

Guichard, D., Koblitz, N., and Keisler, H. J.: Calculus: Early Transcendentals, D. Guichard, 2013.

Haario, H., Saksman, E., and Tamminen, J.: An adaptive metropolis algorithm. Bernoulli 7 223–242, Mathematical Reviews (MathSciNet): MR1828504 Digital Object Identifier: doi, 10, 3318 737, 2001.

Hammitt, J. K. and Shlyakhter, A. I.: The expected value of information and the probability of surprise, Risk Analysis, 19, 135–152, 1999.

Harney, H. L.: Bayesian inference: Parameter estimation and decisions, Springer Science & Business Media, 2013.

Hennig, C. and Kutlukaya, M.: Some Thoughts About the Design of Loss Functions, REVSTAT - Statistical Journal, 5, 19–39, 2007.

Jaynes, E. T.: Probability theory: The logic of science, Cambridge university press, 2003.

Lajaunie, C., Courrioux, G., and Manuel, L.: Foliation fields and 3D cartography in geology: principles of a method based on potential interpolation, Mathematical Geology, 29, 571–584, 1997.

Lark, R., Mathers, S., Thorpe, S., Arkley, S., Morgan, D., and Lawrence, D.: A statistical assessment of the uncertainty in a 3-D geological framework model, Proceedings of the Geologists' Association, 124, 946–958, 2013.

Lindsay, N., Murphy, F., Walsh, J., and Watterson, J.: Outcrop studies of shale smears on fault surfaces, The Geological Modelling of Hydrocarbon Reservoirs and Outcrop Analogues, pp. 113–123, 1993.

Liu, C., McVay, D. A., et al.: Continuous reservoir-simulation-model updating and forecasting improves uncertainty quantification, SPE Reservoir Evaluation & Engineering, 13, 626–637, 2010.

Ma, X., Al-Harbi, M., Datta-Gupta, A., Efendiev, Y., et al.: A multistage sampling method for rapid quantification of uncertainty in history matching geological models, in: SPE Annual Technical Conference and Exhibition, Society of Petroleum Engineers, 2006.

McLane, M., Gouveia, J., Citron, G. P., MacKay, J., and Rose, P. R.: Responsible reporting of uncertain petroleum reserves, AAPG Bulletin, 92, 1431–1452, 2008.

Morton-Thompson, D., Woods, A. M., et al.: Development Geology Reference Manual: AAPG Methods in Exploration Series, No. 10, 10, AAPG, 1993.

Moyé, L. A.: Statistical reasoning in medicine: the intuitive P-value primer, Springer Science & Business Media, 2006.

Mudford, B. et al.: Valuing and comparing oil and gas opportunities: A comparison of decision tree and simulation methodologies, in: SPE Annual Technical Conference and Exhibition, Society of Petroleum Engineers, 2000.

Murtha, J. A. et al.: Monte Carlo simulation: its status and future, Journal of Petroleum Technology, 49, 361–373, 1997.

Randle, C. H., Bond, C. E., Lark, R. M., and Monaghan, A. A.: Uncertainty in geological interpretations: Effectiveness of expert elicitations, Geosphere, 15, 108–118, 2019.

Salvatier, J., Wiecki, T. V., and Fonnesbeck, C.: Probabilistic programming in Python using PyMC3, PeerJ Computer Science, 55, 2016.

Smalley, P. C., Begg, S. H., Naylor, M., Johnsen, S., and Godi, A.: Handling risk and uncertainty in petroleum exploration and asset management: An overview, AAPG Bulletin, 92, 1251–1261, 2008.

Thore, P., Shtuka, A., Lecour, M., Ait-Ettajer, T., and Cognot, R.: Structural uncertainties: Determination, management, and applications, Geophysics, 67, 840–852, 2002.

Verschelde, J.: Programming Tools and File Management - Part I: A Tour of Python, http://homepages.math.uic.edu/~jan/mcs275/mcs275notes/index.html, last visited on 18/10/2017, 2017.

Wadsley, A. W. et al.: Markov Chain Monte Carlo Methods for Reserves Estimation, in: International Petroleum Technology Conference, International Petroleum Technology Conference, 2005.

Wald, A.: Statistical decision functions., 1950.

Weisstein, E. W.: Saddle Point. From MathWorld—A Wolfram Web Resource, http://mathworld.wolfram.com/SaddlePoint.html, last visited on 18/10/2017, 2017.

Wellmann, F. and Caumon, G.: 3-D Structural geological models: Concepts, methods, and uncertainties, 2018.

Wellmann, J. F. and Regenauer-Lieb, K.: Uncertainties have a meaning: Information entropy as a quality measure for 3-D geological models, Tectonophysics, 526, 207–216, 2012.

Wellmann, J. F., Horowitz, F. G., Schill, E., and Regenauer-Lieb, K.: Towards incorporating uncertainty of structural data in 3D geological inversion, Tectonophysics, 490, 141–151, 2010.

Wellmann, J. F., de la Varga, M., Murdie, R. E., Gessner, K., and Jessell, M.: Uncertainty estimation for a geological model of the Sandstone greenstone belt, Western Australia – insights from integrated geological and geophysical inversion in a Bayesian inference framework, in: Characterization of Ore-Forming Systems from Geological, Geochemical and Geophysical Studies, edited by Gessner, K., Glessinkop, T. G., and Sorjonen-Ward, P., Geological Society, London, Special Publications, 453, https://doi.org/https://doi.org/10.1144/SP453.12, 2017.

Wellmann, J. F., de la Varga, M., Murdie, R. E., Gessner, K., and Jessell, M.: Uncertainty estimation for a geological model of the Sandstone greenstone belt, Western Australia–insights from integrated geological and geophysical inversion in a Bayesian inference framework, Geological Society, London, Special Publications, 453, 41–56, 2018.

Wim, J., Swinkels, H., et al.: Guidelines for the evaluation of petroleum reserves and resources, Society of Petroleum Engineers, 2001.

Yielding, G.: Using probabilistic shale smear modelling to relate SGR predictions of column height to fault-zone heterogeneity, Petroleum Geoscience, 18, 33–42, 2012.

Yielding, G., Freeman, B., and Needham, D. T.: Quantitative fault seal prediction, AAPG bulletin, 81, 897–917, 1997.